A Computational Study of HIV Infection Model using Galerkin and Wavelet Collocation Method

Attaullah[a,*], Muhammad Sohaib[a]

[a]*Department of Mathematics & Statistics, Bacha Khan University Charsadda 24461, Pakistan*

Abstract

In this work we implement two numerical schemes namely continuous Galerkin-Petrov (cGP(2)) and Legendre Wavelet Collocation Method (LWCM) for the approximate solution of the mathematical model which describes the behavior of $CD4^+$ T-cells, infected $CD4^+$ T-cells and free HIV virus particles after HIV infection. The present study discuss and analyse the effect of constant and different variable source terms (depending on the viral load) used for the supply of new $CD4^+$ T-cells from thymus on the dynamics of $CD4^+$ T-cells, infected $CD4^+$ T-cells and free HIV virus. Furthermore, the model is also solve using fourth order Runge Kutta (RK4) method. Finally, the validity and reliability of the proposed schemes are verified by comparing the numerical and graphical results with the results of RK4-method. Comparison of the numerical and graphical results of cGP(2) and LWCM with RK4-method confirmed that cGP(2) and LWCM performs excellent accuracy. The present study highlights the accuracy and efficiency of the proposed schemes with the other traditional schemes such as the Laplace Adomian Decomposition Method (LADM), Variational Iteration Method (VIM), Homotopy Analysis Method (HAM), Homotopy Perturbation Method (HPM), Genetic Algorithm (GA), Interior Point Algorithm (IPA), Active Set Algorithm (ASA), Multistep Laplace Adomian Decomposition Method (MSLADM) etc.

Keywords: AIDS; $CD4^+$ T-cells; HIV; cGP(2); LWCM; RK4-method.

1. Introduction

Infectious diseases also known as communicable diseases have long been recognized as a continuous threat to human beings all over the world. Communicable diseases are the diseases transferable from animals to humans, from humans to humans, or from human to animals. The spread occurs abundantly via bacteria, airborne viruses, and through body fluids, e.g., urine, spit, blood, breast milk, tears and so on. Acquired immunodeficiency syndrome (AIDS) is a communicable disease and human immunodeficiency virus (HIV) is the causative agent for AIDS which damages ability of body to fight against diseases and leave it open to attack from usual innocuous infections. On entering the body HIV infects a large amount of $CD4^+$ T-cells and replicates quickly. During this first stage of infection the blood contains high loads of HIV virus particles which spreads throughout the body. HIV viruses spread through bodily fluids, e.g., urine, spit, breast milk, blood, tears and so on. Within these bodily fluids, HIV is present as both free virus particles and virus within infected immune cells. HIV is a retrovirus, in humans $CD4^+$ T-cells lymphocytes are the target of HIV and these are the most abundant white blood cells of the immune system. Because of the central role of

---

*Corresponding author; atta.math786@gmail.com, attaullah@bkuc.edu.pk

CD4$^+$ T-cells in immune regulation, their depletion and destruction can have wide spread deleterious effects on the functioning decreasing the resistance of the immune system. In fact, the decline in the number of these cells is used in a clinical as indicator for the stage of AIDS. The distraction of the function of CD4$^+$ T-cells lies at the heart of the immunodeficiency that characterizes AIDS (see [1, 2, 3, 4] for more details). In recent years, several models for human immune system have been established and extensive research has been conducted in the area of HIV infection of CD4$^+$ T-cells to understand HIV dynamics, HIV infection, disease progression and interaction of the immune system with HIV. Mathematical modeling for the spread of communicable diseases has an increasing influence on the practice and theory of disease control and management [5]. The model for the primary infection with HIV first proposed by Perelson [1] in 1989 and subsequently modified by Perelson et al. [2] using Perelson's model and proved mathematically some of the model's behavior. They observed that the model exhibits many of the symptoms of AIDS seen clinically, i.e., the depletion of CD4$^+$ T-cells, low levels of free virus in the body, and the long latency period etc. They defined the model by considering four compartments: free virus particles, healthy, latently infected and actively infected CD4$^+$ T-cells. They presented dynamics of these compartments by a system of four differential equations. Several models for HIV infection have been developed using the idea of Perelson et al. [2] model which are very important in the field of mathematical modeling of HIV infection. Culshaw and Raun [6] simplify the Perelson [2] model into one consisting of only three components, i.e., the free virus particles, infected and healthy CD4$^+$ T-cells. They introduce a discrete time delay to the model and show the change in time between the expel of virus particles and infection of cells on a cellular level. In literature, a large number of analytical and numerical schemes were employed in order to find out the approximate solution of the HIV infection model (see [7, 8, 9, 10, 11, 12, 13] for details).

The key objective of the present study is to show and analyze the effect of constant and different variable source terms of new CD4$^+$ T-cells from thymus depending on the viral load and compared the influence on the HIV infection model proposed by Malik et al. [11]. We utilized the cGP(2) and LWCM to find out the approximate solution of the proposed model. Furthermore, we solved the model by using classical RK4-method. For validity and reliability of the proposed schemes, we compared the results with those obtained from RK4-method. We also compared the results and absolute error of of the present schemes with other classical schemes used in literature [7, 8, 9, 11, 12] for the model relative to RK4-scheme. Graphical results have been presented and discussed quantitatively to illustrate the solution. The model discussed here focuses on the population of healthy CD4$^+$ T-cells and infected CD4$^+$ T-cells. Throughout the remainder of this article the term healthy T-cells and infected T-cells will use to mean healthy CD4$^+$ T-cells and infected CD4$^+$ T-cells respectively. This article is organized as follows: Section 2 describes the model for HIV infection of healthy T-cells. Section 3 and 4 includes the cGP(2) and LWCM implemented for the proposed model. In Section 5, the results and discussions for the model are presented. Finally, a brief conclusion of the study is given in Section 6.

2. The HIV Infection Model Description

Mathematical models have become important tools in the area of HIV infection of healthy T-cells to understand HIV dynamics, HIV infection, disease progression and interaction of the immune system with HIV. The main target of HIV virus in humans are healthy T-cells. Once HIV enters the body, it infects a large amount of healthy T-cells which causes gradual depletion of healthy T-cells. Subsequently the immune system of the body is destabilized, and thus progressively compromises the host's immune response

to opportunistic infections leading to acquired immunodeficiency syndrome (AIDS). Therefore, the decline in the number of these cells is used as a primary indicator in order to measure progression of HIV infection and stages of AIDS. These cells produce at a constant rate s_0 from precursors in the bone marrow and thymus [14]. The transfer diagram is depicted in Figure 1. The model which consist of nonlinear system of
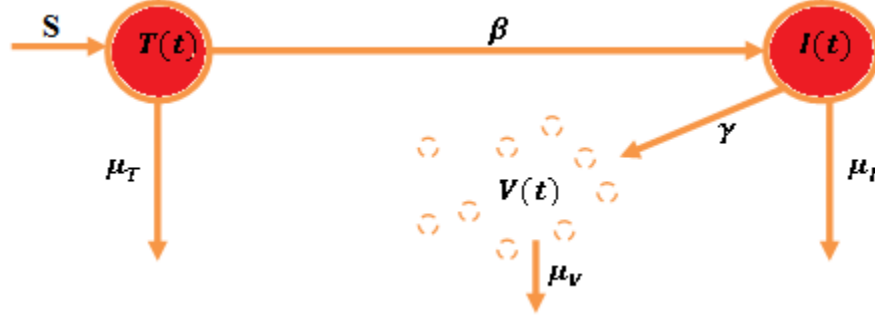

Figure 1: Diagrammatic representation of the mathematical model for HIV infection, where $S = s_0 + \alpha T(t)\left(1 - \frac{T(t)+I(t)}{T_{\max}}\right)$.

ordinary differential equations for HIV infection of healthy T-cells proposed by Malik et al. [11] is:

$$\frac{dT(t)}{dt} = f_1\left(T(t), I(t), V(t)\right) = s_0 - \mu_T T(t) + \alpha T(t)\left(1 - \frac{T(t)+I(t)}{T_{\max}}\right) - \beta V T(t), \tag{2.1}$$

$$\frac{dI(t)}{dt} = f_2\left(T(t), I(t), V(t)\right) = \beta V(t) T(t) - I(t)\mu_I, \tag{2.2}$$

$$\frac{dV(t)}{dt} = f_3\left(T(t), I(t), V(t)\right) = \gamma \mu_I I(t) - \mu_V V(t). \tag{2.3}$$

with the following initial conditions:

$$T(0) = 0.1, \tag{2.4}$$

$$I(0) = 0, \tag{2.5}$$

$$V(0) = 0.1. \tag{2.6}$$

In the above expression T, I and V represent the population of healthy T-cells, infected T-cells and free HIV virus particles in the blood of HIV infected individual respectively. The initial values of these dependent variables and explanation of other parameters with their values involved in the HIV model are given in Table 1

Table 1: List of parameter and variables used in the HIV model

Parameters	Description	Values
s_0	The new supply rate of healthy T-cells from thymus	$0.1 \text{ day}^{-1}\text{mm}^{-3}$
α	Growth rate of healthy T-cells population	3 day^{-1}
μ_T	Turnover rate of healthy T-cells	0.02 day^{-1}
μ_I	Turnover rate of infected T-cells	0.3 day^{-1}
μ_V	Turnover rate of free virus	2.4 day^{-1}
β	The infection rate	0.0027 day^{-1}
$T_{\max}$	Maximum population level of healthy T-cells	1500 mm^{-3}
γ	Number of virus produced by infected T-cells	10 day^{-1}

3

In literature (see [6, 7, 8, 9, 10, 11, 12, 13] for more details) the HIV model proposed with a constant source term for the supply of new healthy T-cells from thymus. But HIV may have the ability to infect T-cells in the bone marrow and thymus on entering into humans body and thus lead to reduced production of new healthy T-cells [2]. For this reason, the HIV model (see [1, 2, 15, 16, 17] for more details) assumed with variable source term for the supply of new healthy T-cells from thymus, i.e, kirschner [15] and Webb et al. [18] consider the source term $s_1 = 0.5s_0 + \frac{5s_0}{1+V(t)}$, Perelson et al. [2] used the source term $s_2 = \frac{s_0\xi}{\xi+V(t)}$, where ξ is constant. If $V = 0$, then s_2 is a constant and will be decreased to half of its normal value if the viral load V(t) increases to the point ξ, and the source term $s_3 = s_0 \exp(-\xi V(t))$ is assumed in Perelson [1] model. Kirschner et al. [16], Hermández [17] and Butler et al. [19] also consider the HIV model with source term like used in Perelson et al. [2] model with $\xi = 1$.

In this work, we consider the HIV model proposed in [11] and show the influence of all these source terms on the dynamical behaviour of healthy T-cells, infected T-cells and free HIV virus particles. Solutions are obtained by using continuous Galerkin Petrov method.

3. The CGP(2) Method for the HIV Infection Model

Nowadays the cGP-method has been successfully employed to solve many types of non linear problems in science and engineering see for example [20, 21, 22, 23, 24, 25, 26]. In this paper, we used this approach to the HIV infection model [11]. The system of ODEs for HIV model (2.1)–(2.3) can considered as:
Find $\mathbf{u} : [0, t_{max}] \to \mathbf{V} = \mathbb{R}^d$ *such that*

$$
\begin{aligned}
d_t\mathbf{u}(t) &= \mathbf{F}(t, \mathbf{u}(t)) \quad \text{for} \quad t \in (0, t_{max}), \\
\mathbf{u}(0) &= \mathbf{u}_0,
\end{aligned}
\tag{3.1}
$$

where $\mathbf{u}(t) = [T(t), I(t), V(t)]$ and $\mathbf{F}$ is the nonlinear right hand side vector valued function. At $t = 0$, $u_1(0) = T(0)$, $u_2(0) = I(0)$ and $u_3(0) = V(0)$, where $T(0)$, $I(0)$ and $V(0)$ are the initial conditions given in Table 1.

In order to find the approximate solution of (3.1), we partitioned the time interval $I := [0, t_{max}]$ into a number of small pieces $I_n := (t_{n-1}, t_n)$, where $n \in \{1, \dots, N\}$ and

$$
0 = t_0 < t_1 < \cdots < t_{N-1} < t_N = t_{max}.
$$

The symbol $\tau = t_n - t_{n-1}$ is used to represent the maximum time step size. For the derivation of the cGP-method, the system of equations in (3.1) is multiplied with a suitable test functions (see [20, 21, 22, 26] for more details) and integrate over I_n. The discrete solution $\mathbf{u}_\tau|_{I_n}$ can be represent by the polynomial ansatz

$$
\mathbf{u}_\tau|_{I_n}(t) := \sum_{j=0}^{k} \mathbf{U}_n^j \phi_{n,j}(t),
\tag{3.2}
$$

where $\mathbf{U}_n^j$ are the members of the function space $\mathbf{V}$ and the basis functions $\phi_{n,j} \in \mathbb{P}_k(I_n)$ can be chosen as Lagrange basis functions w. r. t. the $k+1$ points $t_{n,j} \in I_n$ with the following assumption

$$
\phi_{n,j}(t_{n,i}) = \delta_{i,j}, \qquad i, j = 0, \dots, k
\tag{3.3}
$$

where $\delta_{i,j}$ the usual Kronecker delta. We choose the points as $t_{n,0} = t_{n-1}$ and $t_{n,1}, \dots, t_{n,k}$ the $(k+1)$-quadrature points of Gauß-Lobatto formula on each time interval. In this way, the initial condition can be written as

$$
\mathbf{U}_n^0 = \mathbf{u}_\tau|_{I_{n-1}}(t_{n-1}) \quad \text{if} \quad n \geq 2 \qquad \text{or} \qquad \mathbf{U}_n^0 = \mathbf{u}_0 \quad \text{if} \quad n = 1.
\tag{3.4}
$$

The basis functions $\phi_{n,j} \in \mathbb{P}_k(I_n)$ of (3.2) are defined using the reference transformations (see [20, 21, 22, 26] for more details). Similarly, the test basis functions $\hat{\psi}_i \in \mathbb{P}_{k-1}(\hat{I})$ are defined with appropriate choice in order to compute the coefficients (see [20, 21, 22, 26] for details). Finally, the cGP(k)-method reads:

$$\sum_{j=0}^{k} \alpha_{i,j} \mathbf{U}_n^j = \frac{\tau_n}{2} \left\{ \mathbf{F}(t_{n,i}, \mathbf{U}_n^i) + \beta_i \mathbf{F}(t_{n,0}, \mathbf{U}_n^0) \right\} \quad \forall \ i = 1, 2, 3, \cdots, k, \tag{3.5}$$

where $\mathbf{U}_n^0 = \mathbf{U}_{n-1}^k$ for $n > 1$ and $\mathbf{U}_1^0 = \mathbf{u}_0$ for $n = 1$, are the initial values and $\alpha_{i,j}$ and β_i are defined are

$$\alpha_{i,j} = \hat{\varphi}_j'(\hat{t}_i) + \beta_i \hat{\varphi}_j'(\hat{t}_0), \quad t_{n,u} = \omega_n(\hat{t}_\mu) \text{ and } \beta_i = \hat{w}_0 \hat{\psi}_i(\hat{t}_0). \tag{3.6}$$

Once the above system is solved, the initial condition for the next time interval $\bar{I}_{n+1}$ is set to $\mathbf{U}_{n+1}^0 = \mathbf{U}_n^k$. For $k = 2$, the coefficients $\alpha_{i,j}$ and $\beta_{i,j}$ of the cGP(2)-method are computed as follows:

3.1. The cGP(2) method

Three-point Gauß-Lobatto formula (Simpson rule) is used to define the quadratic basis functions with weights $\hat{w}_0 = \hat{w}_2 = 1/3$, $\hat{w}_1 = 4/3$ and $\hat{t}_0 = -1$, $\hat{t}_1 = 0$, $\hat{t}_2 = 1$. Then, we get

$$\alpha_{i,j} = \begin{pmatrix} -\frac{5}{4} & 1 & \frac{1}{4} \\ 2 & -4 & 2 \end{pmatrix}, \quad \beta_i = \begin{pmatrix} \frac{1}{2} \\ -1 \end{pmatrix}, \quad i = 1, 2, \quad j = 0, 1, 2.$$

Thus, the system to be solved for $\mathbf{U}_n^1, \mathbf{U}_n^2 \in \mathbf{V}$ from the known $\mathbf{U}_n^0 = \mathbf{U}_{n-1}^2$ becomes:

$$\alpha_{1,1} \mathbf{U}_n^1 + \alpha_{1,2} \mathbf{U}_n^2 = -\alpha_{1,0} \mathbf{U}_n^0 + \frac{\tau_n}{2} \left\{ \mathbf{F}(t_{n,1}, \mathbf{U}_n^1) + \beta_1 \mathbf{F}(t_{n,0}, \mathbf{U}_n^0) \right\}, \tag{3.7}$$

$$\alpha_{2,1} \mathbf{U}_n^1 + \alpha_{2,2} \mathbf{U}_n^2 = -\alpha_{2,0} \mathbf{U}_n^0 + \frac{\tau_n}{2} \left\{ \mathbf{F}(t_{n,2}, \mathbf{U}_n^2) + \beta_2 \mathbf{F}(t_{n,0}, \mathbf{U}_n^0) \right\}, \tag{3.8}$$

where $\mathbf{U}_n^0$ represent the initial condition at the current time interval.

4. Description of LWCM for HIV Infection Model

Wavelet has wide spread application in many areas of science and engineering. During last two decades the use of wavelet in approximation theory is very popular. In this section we use LWCM which uses Legendre polynomials as a basis function. The unknown function is approximated with Legendre wavelet. The collocation points are used to obtain the system of algebraic equations. The algebraic equations are solved with the help of Mathematica software. The important feature of Legendre wavelet is it orthogonality due to which coefficient of expansion are easily calculated. Another main advantage of the using wavelets method is the sparsity of the coefficient matrix of the final system of equations. LWCM is successfully applied to ordinary differential equations [27], partial differential equations [28], fractional differential equations [29], and fractional partial differential equations [30].

4.1. Legendre wavelet

The Legendre wavelet [31] is defined on [0,1) and is given by

$$\psi_{n,m}(t) = \begin{cases} \sqrt{m + \frac{1}{2}} \ 2^{\frac{k}{2}} \ P_m(2^k t - 2n + 1), & \frac{n-1}{2^{k-1}} \le t \le \frac{n}{2^{k-1}}, \\ 0, & \textbf{otherwise} \end{cases} \tag{4.1}$$

5

where $n = 1, 2, 3, \cdots, 2^{k-1}$, $m = 0, 1, 2, 3, \cdots, M-1$, the coefficient $\sqrt{m + \frac{1}{2}}$ is for orthonormality, and k, M are positive integers. $P_m(t)$ are the Legendre polynomials of order m which are defined on the interval [-1, 1] and is given by the following recurrence relations

$$P_0(t) = 1,$$

$$P_1(t) = t,$$

$$P_{m+1}(t) = \left(\frac{2m+1}{m+1} \right) t P_m(t) - \left(\frac{m}{m+1} \right) P_{m-1}(t), \qquad m = 1, 2, 3 \cdots$$

The Legendre wavelet form an orthonormal basis for $L^2(R)$, so we can approximate a function as a linear combination of Legendre wavelet.

4.2. Methodology of LWCM

In this section we apply the LWCM to the model given by Eq. (2.1)-(2.6). According to LWCM

$$T(t) = \sum_{n=1}^{2^{k-1}} \sum_{m=0}^{M-1} a_{n,m} \psi_{n,m}(t) = \mathbf{A}\psi(t), \qquad (4.2)$$

$$I(t) = \sum_{n=1}^{2^{k-1}} \sum_{m=0}^{M-1} b_{n,m} \psi_{n,m}(t) = \mathbf{B}\psi(t), \qquad (4.3)$$

$$V(t) = \sum_{n=1}^{2^{k-1}} \sum_{m=0}^{M-1} c_{n,m} \psi_{n,m}(t) = \mathbf{C}\psi(t). \qquad (4.4)$$

The nonlinear terms are approximated as:

$$T^2(t) = \sum_{n=1}^{2^{k-1}} \sum_{m=0}^{M-1} d_{n,m} \psi_{n,m}(t) = \mathbf{D}\psi(t), \qquad (4.5)$$

$$T(t)I(t) = \sum_{n=1}^{2^{k-1}} \sum_{m=0}^{M-1} e_{n,m} \psi_{n,m}(t) = \mathbf{E}\psi(t), \qquad (4.6)$$

$$V(t)T(t) = \sum_{n=1}^{2^{k-1}} \sum_{m=0}^{M-1} f_{n,m} \psi_{n,m}(t) = \mathbf{F}\psi(t), \qquad (4.7)$$

where A, B, C, D, E, F, and ψ are $2^{k-1}M \times 1$ matrices given by:

$$A = \left[a_{1,0}, \cdots, a_{1,M-1}, a_{2,0}, \cdots, a_{2,M-1}, \cdots, a_{2^{k-1},0}, \cdots, a_{2^{k-1},M-1} \right],$$

$$B = \left[b_{1,0}, \cdots, b_{1,M-1}, b_{2,0}, \cdots, b_{2,M-1}, \cdots, b_{2^{k-1},0}, \cdots, b_{2^{k-1},M-1} \right],$$

6

$$C = \left[c_{1,0}, \cdots, c_{1,M-1}, c_{2,0}, \cdots, c_{2,M-1}, \cdots, c_{2^{k-1},0}, \cdots, c_{2^{k-1},M-1} \right],$$

$$D = \left[d_{1,0}, \cdots, d_{1,M-1}, d_{2,0}, \cdots, d_{2,M-1}, \cdots, d_{2^{k-1},0}, \cdots, d_{2^{k-1},M-1} \right],$$

$$E = \left[e_{1,0}, \cdots, e_{1,M-1}, e_{2,0}, \cdots, e_{2,M-1}, \cdots, e_{2^{k-1},0}, \cdots, e_{2^{k-1},M-1} \right],$$

$$F = \left[f_{1,0}, \cdots, f_{1,M-1}, f_{2,0}, \cdots, f_{2,M-1}, \cdots, f_{2^{k-1},0}, \cdots, f_{2^{k-1},M-1} \right],$$

$$\psi(t) = \left[\psi_{1,0}, \cdots, \psi_{1,M-1}, \psi_{2,0}, \cdots, \psi_{2,M-1}, \cdots, \psi_{2^{k-1},0}, \cdots, \psi_{2^{k-1},M-1} \right]^T.$$

Using Eq. (4.2)–(4.7) in Eq. (2.1)–(2.6) we obtained the following equations:

$$A^T \psi'(t) = s_0 + \mu_T A^T \psi(t) + \alpha A^T \psi(t) - \frac{\alpha}{T_{\max}} \left(D^T \psi(t) + E^T \psi(t) \right) - \beta F^T \psi(t), \qquad (4.8)$$

$$B^T \psi'(t) = \beta F^T \psi(t) - B^T \psi(t) \mu_I, \qquad (4.9)$$

$$C^T \psi'(t) = \gamma \mu_I B^T \psi(t) - \mu_V C^T \psi(t), \qquad (4.10)$$

$$A^T \psi(0) = 0.1, \qquad (4.11)$$

$$B^T \psi(0) = 0, \qquad (4.12)$$

$$C^T \psi(0) = 0.1. \qquad (4.13)$$

Now collocating Eq. (4.8)-(4.10) and Eq. (4.5)-(4.7) at

$$t_j = \frac{j - 0.5}{2^{k-1} M},$$

where $\left(j = 1, 2, 3, \cdots 2^{k-1} M - 1 \right)$ for Eq. (4.8)-(4.10) and $\left(j = 1, 2, 3, \cdots 2^{k-1} M \right)$ for Eq. (4.5)-(4.7) we obtained the following equations:

$$A^T \psi'(t_j) = s_0 + \mu_T A^T \psi(t_j) + \alpha A^T \psi(t_j) - \frac{\alpha}{T_{\max}} \left(D^T \psi(t_j) + E^T \psi(t_j) \right) - \beta F^T \psi(t_j), \qquad (4.14)$$

$$B^T \psi'(t_j) = \beta F^T \psi(t_j) - B^T \psi(t_j) \mu_I, \qquad (4.15)$$

$$C^T \psi'(t_j) = \gamma \mu_I B^T \psi(t_j) - \mu_V C^T \psi(t_j), \qquad (4.16)$$

$$T^2(t_j) = D^T \psi(t_j), \qquad (4.17)$$

$$T(t_j) I(t_j) = E^T \psi(t_j), \qquad (4.18)$$

$$V(t_j) T(t_j) = F^T \psi(t_j). \qquad (4.19)$$

From Eq. (4.2)–(4.7) it is clear that there are total $6(2^{k-1} M)$ unknown constants. To find out these constants we need $6(2^{k-1} M)$ equations out of which $6(2^{k-1} M) - 3$ equations are obtained from Eq. (4.14)–(4.19) while remaining three equations are obtained from Eq. (4.11)–(4.13). Solving the system of equations will give the unknown constants which upon using in Eq. (4.2)–(4.4) will give the desire solution.

5. Results and Discussion

In this section, the simulation results illestrate graphically and numerically carried out by cGP(2) and LWCM. The parameters values and initial conditions used in the numerical simulations are given in Table 1. The population dynamics of healthy T-cells, infected T-cells and free HIV virus particles with constant and different variable source terms are presented in Figure 2a–2c. The graph of $T(t)$, $I(t)$ and $V(t)$ shows a decaying oscillatory behaviour but their are only a slightly difference in their population dynamics using different source terms i.e., constant and variable (depending on viral load). From Figure 2a, it could be seen that the population dynamic of healthy T-cells for s_1, behaves different from s_0, s_2 and s_3 throughout the time period of seventy days while for some time s_2 and s_3 follows considerably the same dynamics as like constant source term. But after some time their are observable changes appear in their dynamics. Similarly, the influence of these source terms show same behavior for the population dynamics of infected T-cells and free HIV virus particles like for healthy T-cells as shown in Figures 2b–2c. The phase diagram of $I(t)$–$T(t)$, $V(t)$–$T(t)$, $V(t)$–$I(t)$ and $V(t)$–$I(t)$–$T(t)$ for HIV infection model are presented in Figures 2d–2g. For all source term, the HIV infection model exhibit chaotic behavior. Initially, the results overlap over each other and after some time they show different behavior in their dynamics in phase diagrams. Although every phase diagram has numerically individual meaning at every point and not focus on the detail medical interpretation of figures related to solution. Additionally, we utilized the RK4-method to the HIV infection model and obtained its numerical solution. We compared the numerical solutions of cGP(2) and LWCM with RK4-method. Furthermore, we also compared the results and absolute errors of the proposed schemes with other conventional method, i.e., HPM [7], LADM [8] MVIM [32], VIM [12], Bessel collocation [9], GA [11], IPA [11], ASA [11], GA-IPA [11] and GA-ASA [11] relative to RK4-method given in Tables 2–10 for $T(t)$, $I(t)$ and $V(t)$ respectively. After comparison it could be clearly observed that the proposed schemes provides a quite accurate results as compared to other methods used for the model. The results of the presents methods are very close to RK4-methods. For more concerns, we illustrated the graphical results of both techniques through Figures 2h–2j relative to RK4-method. The results obtained through cGP(2) and LWCM are in fairly good accuracy with RK4-method. So it depicts the accuracy and validity of the proposed methods, as both results clearly overlap each other throughout the time period of seventy days.

From the graphical results in Figures 2h–2j and numerical results presented in Tables 2–10 clearly expose that the proposed techniques provide the results of the HIV infection model in a reasonably good agreement with the results obtained by RK4-method which implies that the cGP(2) and LWCM can predict the behavior of these variables accurately for the region under consideration.
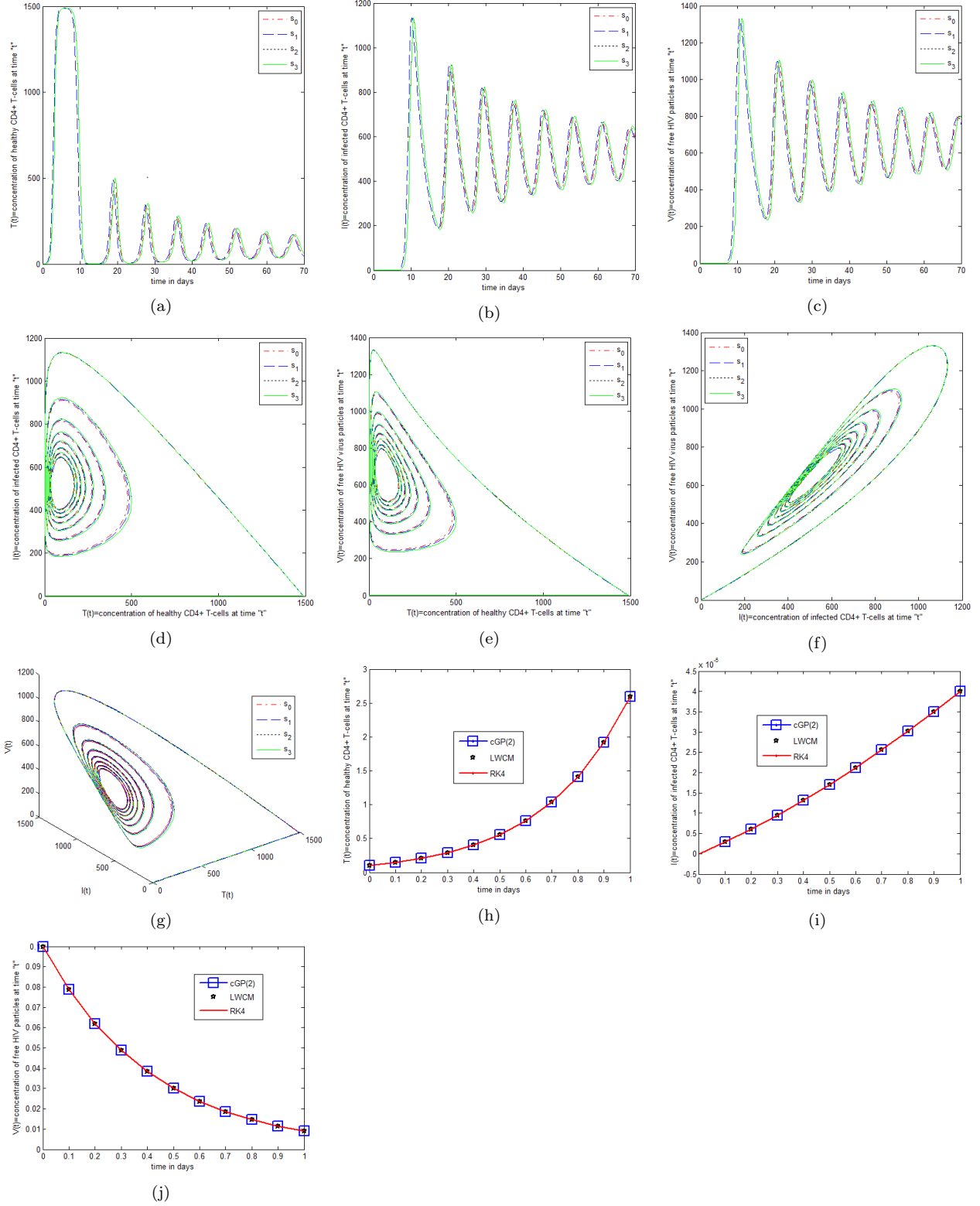
Figure 2: The influence of constant and different variable source terms of new healthy T-cells depending on the concentration of virus from thymus on HIV infection model, phase plot of $I(t)$–$T(t)$, $V(t)$–$T(t)$, $V(t)$–$I(t)$, $V(t)$–$I(t)$–$T(t)$ for 70 days and graphical comparison between the results of cGP(2)-method and RK4-method for $T(t)$, $I(t)$ and $V(t)$ for 10 days

9

Table 2: Comparison of numerical solutions for $T(t)$ between the proposed schemes and classical methods

t_i	GA [11]	IPA [11]	ASA [11]	GA-IPA [11]	GA-ASA [11]	RK4	cGP(2)	LWCM
0.0	0.100000000	0.100000000	0.100000000	0.100000000	0.100000000	0.100000000	0.100000000	0.100000000
0.1	0.145758404	0.145782503	0.145782636	0.145782500	0.145782579	0.146356333	0.146358492	0.146359154
0.2	0.207342243	0.207410504	0.207411437	0.207410481	0.207411152	0.208800678	0.208806496	0.208808176
0.3	0.291230014	0.291379572	0.291381169	0.291379533	0.291380703	0.292914452	0.292926206	0.292929539
0.4	0.404593848	0.404877886	0.404879762	0.404877840	0.404879224	0.406213674	0.406234784	0.406240711
0.5	0.556827606	0.557321160	0.557323063	0.557321112	0.557322519	0.558818129	0.558853667	0.558863585
0.6	0.761074981	0.761887565	0.761889589	0.761887514	0.761889002	0.764350814	0.764408244	0.764424204
0.7	1.035757595	1.037052658	1.037055277	1.037052593	1.037054502	1.041146025	1.041236244	1.041261233
0.8	1.406103102	1.408124304	1.408128242	1.408124206	1.408127066	1.413870248	1.414009061	1.414047408
0.9	1.905673283	1.908777600	1.908783521	1.908777453	1.908781756	1.915693859	1.915904055	1.915961934
1.0	2.577892152	2.582589801	2.582597835	2.582589601	2.582595457	2.591195190	2.591509458	2.591593521

Table 3: Comparison of numerical solutions for $I(t)$ between the proposed schemes and classical methods

t_i	GA [11]	IPA [11]	ASA [11]	GA-IPA [11]	GA-ASA [11]	RK4	cGP(2)	LWCM
0.0	0.0000E+00	0.0000E+00	0.0000E+00	0.0000E+00	0.0000E+00	0.0000E+00	0.0000E+00	-2.8562E-21
0.1	4.2247E-06	3.0007E-06	2.6081E-06	2.9975E-06	2.8253E-06	2.8645E-06	2.8648E-06	2.8649E-06
0.2	2.8356E-06	7.6675E-06	7.2513E-06	7.6939E-06	7.7601E-06	6.0318E-06	6.0325E-06	6.0327E-06
0.3	1.7185E-06	1.2065E-05	1.1876E-05	1.2114E-05	1.2455E-05	9.4700E-06	9.4711E-06	9.4713E-06
0.4	3.5927E-06	1.5563E-05	1.5702E-05	1.5614E-05	1.6089E-05	1.3156E-05	1.3157E-05	1.3158E-05
0.5	8.8488E-06	1.8423E-05	1.8837E-05	1.8457E-05	1.8891E-05	1.7076E-05	1.7078E-05	1.7078E-05
0.6	1.6386E-05	2.1373E-05	2.1891E-05	2.1386E-05	2.1664E-05	2.1220E-05	2.1223E-05	2.1223E-05
0.7	2.4450E-05	2.5200E-05	2.5594E-05	2.5200E-05	2.5311E-05	2.5585E-05	2.5589E-05	2.5589E-05
0.8	3.1472E-05	3.0326E-05	3.0413E-05	3.0332E-05	3.0358E-05	3.0172E-05	3.0176E-05	3.0177E-05
0.9	3.6904E-05	3.6391E-05	3.6166E-05	3.6416E-05	3.6478E-05	3.4985E-05	3.4989E-05	3.4990E-05
1.0	4.2058E-05	4.1842E-05	4.1638E-05	4.1873E-05	4.2012E-05	4.0031E-05	4.0036E-05	4.0037E-05

Table 4: Comparison of numerical solutions for $V(t)$ between the proposed schemes and classical methods

t_i	GA [11]	IPA [11]	ASA [11]	GA-IPA [11]	GA-ASA [11]	RK4	cGP(2)	LWCM
0.0	0.100000000	0.100000000	0.100000000	0.100000000	0.100000000	0.100000000	0.100000000	0.100000000
0.1	0.078656981	0.078656268	0.078656409	0.078656271	0.078656368	0.078663814	0.078663263	0.078663176
0.2	0.061861944	0.061866671	0.061864908	0.061866656	0.061865211	0.061880847	0.061879980	0.061879843
0.3	0.048661037	0.048671537	0.048668574	0.048671515	0.048669164	0.048679673	0.048678650	0.048678489
0.4	0.038284555	0.038298310	0.038295736	0.038298301	0.038296384	0.038296130	0.038295057	0.038294887
0.5	0.030121829	0.030135659	0.030134687	0.030135674	0.030135171	0.030129095	0.030128040	0.030127874
0.6	0.023696108	0.023707580	0.023708379	0.023707619	0.023708600	0.023705703	0.023704707	0.023704550
0.7	0.018639444	0.018647508	0.018649133	0.018647554	0.018649149	0.018653978	0.018653065	0.018652920
0.8	0.014667578	0.014672419	0.014673341	0.014672451	0.014673322	0.014681314	0.014680493	0.014680363
0.9	0.011554820	0.011556941	0.011556164	0.011556949	0.011556283	0.011557535	0.011556808	0.011556693
1.0	0.009108938	0.009107460	0.009106245	0.009107464	0.009106480	0.009101579	0.009100944	0.009100818

Table 5: Comparison of numerical solutions for $T(t)$ between the proposed schemes and classical methods

t_i	0.0	0.2	0.4	0.6	0.8	1.0
LWCM	0.1000000000	0.2088081767	0.4062407112	0.7644242042	1.4140474083	2.5915935217
cGP(2) method	0.1000000000	0.2088064964	0.4062347843	0.7644082444	1.4140090611	2.5915094589
GA [11]	0.1000000000	0.2073422431	0.4045938486	0.7610749817	1.4061031024	2.5778921524
IPA [11]	0.1000000000	0.2074105042	0.4048778868	0.7618875655	1.4081243044	2.5825898013
ASA [11]	0.1000000000	0.2074114374	0.4048797626	0.7618895893	1.4081282422	2.5825978353
GA-IPA [11]	0.1000000000	0.2074104817	0.2074104817	0.2074104817	0.2074104817	0.2074104817
GA-ASA [11]	0.1000000000	0.2074111526	0.4048792244	0.7618890022	1.4081270663	2.5825954577
LADM [8]	0.1000000000	0.2088073298	0.4061358315	0.7624762220	1.3980828630	2.5078741510
LADM-Padé [8]	0.1000000000	0.2088072731	0.4061052625	0.7611467713	1.3773198590	2.3291697610
VIM [12]	0.1000000000	0.2088073214	0.4061346587	0.7624530350	1.3978805880	2.5067466690
MVIM [12]	0.1000000000	0.2088080868	0.4062407949	0.7644287245	1.4140941730	2.5919210760
HPM [7]	0.1000000000	0.2088073294	0.4061358277	0.7624762056	1.3980828100	2.5078740100
Bessel [9]	0.1000000000	0.2038616561	0.3803309335	0.6954623767	1.2759624442	2.3832277428
RK4 method	0.1000000000	0.2088006788	0.4062136749	0.7643508145	1.4138702489	2.5911951903

Table 6: Comparison of numerical solutions for $I(t)$ between the proposed schemes and classical methods

t_i	0.0	0.2	0.4	0.6	0.8	1.0
LWCM	-2.85625E-21	6.03271E-06	1.31583E-05	2.12238E-05	3.01774E-05	4.00378E-05
cGP(2) method	0.00000E+00	6.03254E-06	1.31579E-05	2.12231E-05	3.01764E-05	4.00364E-05
GA [11]	0.00000E+00	2.83561E-06	3.59276E-06	1.63861E-05	3.14727E-05	4.20582E-05
IPA [11]	0.00000E+00	7.66752E-06	1.55638E-05	2.13739E-05	3.03260E-05	4.18421E-05
ASA [11]	0.00000E+00	7.25138E-06	1.57029E-05	2.18911E-05	3.04139E-05	4.16383E-05
GA-IPA [11]	0.00000E+00	7.69390E-06	1.56145E-05	2.13863E-05	3.03320E-05	4.18740E-05
GA-ASA [11]	0.00000E+00	7.76013E-06	1.60895E-05	2.16643E-05	3.03590E-05	4.20128E-05
LADM [8]	0.00000E+00	6.03270E-06	1.31589E-05	2.12329E-05	3.02427E-05	4.03332E-05
LADM-Padé [8]	0.00000E+00	6.03270E-06	1.31591E-05	2.12683E-05	3.00691E-05	3.98736E-05
VIM [12]	0.00000E+00	6.03263E-06	1.31487E-05	2.10141E-05	2.79513E-05	2.43156E-05
MVIM [12]	1.00000E-13	6.03270E-06	1.31583E-05	2.12233E-05	3.01745E-05	4.00254E-05
HPM [7]	0.00000E+00	6.03270E-06	1.31589E-05	2.12329E-05	3.02427E-05	4.03332E-05
Bessel [9]	0.00000E+00	6.24787E-06	1.29355E-05	2.03526E-05	2.83730E-05	3.69084E-05
RK4 method	0.00000E+00	6.03187E-06	1.31564E-05	2.12206E-05	3.01728E-05	4.00314E-05

Table 7: Comparison of numerical solutions for $V(t)$ between the proposed schemes and classical methods

t_i	0.0	0.2	0.4	0.6	0.8	1.0
LWCM	0.1000000000	0.0618798436	0.0382948879	0.0237045502	0.0146803638	0.0091008183
cGP(2)-method	0.1000000000	0.0618799805	0.0382950575	0.0237047074	0.0146804932	0.0091009447
GA [11]	0.1000000000	0.0618619447	0.0382845550	0.0236961083	0.0146675785	0.0091089381
IPA [11]	0.1000000000	0.0618666712	0.0382983109	0.0237075809	0.0146724192	0.0091074600
ASA [11]	0.1000000000	0.0618649088	0.0382957364	0.0237083794	0.0146733410	0.0091062452
GA-IPA [11]	0.1000000000	0.0618666565	0.0382983011	0.0237076190	0.0146724517	0.0091074649
GA-ASA [11]	0.1000000000	0.0618652111	0.0382963843	0.0237086009	0.0146733229	0.0091064801
LADM [8]	0.1000000000	0.0618799531	0.0383081805	0.0239198161	0.0162123434	0.0160550224
LADM-Padé [8]	0.1000000000	0.0618799603	0.0383132488	0.0243917435	0.0099672189	0.0033050764
VIM [12]	0.1000000000	0.0618799531	0.0383082013	0.0239202926	0.0162170455	0.0160841871
MVIM [12]	0.1000000000	0.0618799088	0.0382959577	0.0237102948	0.0147004190	0.0091572387
HPM [7]	0.1000000000	0.0618799531	0.0383081805	0.0239198161	0.0162123434	0.0160550224
Bessel [9]	0.1000000000	0.0618799186	0.0382949349	0.0237043186	0.0146795698	0.0237043186
RK4 method	0.1000000000	0.0618808474	0.0382961304	0.0237057031	0.0146813143	0.0091015790

Table 8: Comparison of absolute errors for $T(t)$ of the proposed schemes and classical methods relative to RK4 method

t_i	0.0	0.2	0.4	0.6	0.8	1.0
LWCM	2.78E-17	7.50E-06	2.70E-05	7.34E-05	1.77E-04	3.98E-04
cGP(2)-method	0.00E+00	5.81E-06	2.11E-05	5.74E-05	1.38E-04	3.14E-04
GA [11]	0.00E+00	1.39E-03	1.35E-03	2.50E-03	5.85E-03	8.88E-03
IPA [11]	0.00E+00	1.32E-03	1.06E-03	1.69E-03	3.83E-03	4.19E-03
ASA [11]	0.00E+00	1.32E-03	1.06E-03	1.69E-03	3.83E-03	4.18E-03
GA-IPA [11]	0.00E+00	1.32E-03	1.06E-03	1.69E-03	3.83E-03	4.19E-03
GA-ASA [11]	0.00E+00	1.32E-03	1.06E-03	1.69E-03	3.83E-03	4.18E-03
LADM [8]	0.00E+00	7.78E-05	1.95E-04	1.10E-03	1.39E-02	7.89E-02
LADM-Padé [8]	0.00E+00	7.77E-05	1.65E-04	2.43E-03	3.46E-02	2.58E-01
VIM [12]	0.00E+00	7.78E-05	1.94E-04	1.13E-03	1.41E-02	8.00E-02
MVIM [12]	0.00E+00	7.85E-05	3.00E-04	8.49E-04	2.14E-03	5.14E-03
HPM [7]	0.00E+00	7.78E-05	1.95E-04	1.10E-03	1.39E-02	7.89E-02
Bessel [9]	0.00E+00	4.87E-03	2.56E-02	6.81E-02	1.36E-01	2.04E-01

Table 9: Comparison of absolute errors for $I(t)$ of the proposed schemes and classical methods relative to RK4-method

t_i	0.0	0.2	0.4	0.6	0.8	1.0
LWCM	2.86E-21	8.36E-10	1.95E-09	3.20E-09	4.63E-09	6.44E-09
cGP(2)-method	0.00E+00	6.67E-10	1.49E-09	2.48E-09	3.65E-09	5.04E-09
GA [11]	0.00E+00	3.20E-06	9.56E-06	4.82E-06	1.32E-06	2.06E-06
IPA [11]	0.00E+00	1.64E-06	2.41E-06	1.63E-07	1.74E-07	1.85E-06
ASA [11]	0.00E+00	1.22E-06	2.55E-06	6.81E-07	2.62E-07	1.64E-06
GA-IPA [11]	0.00E+00	1.66E-06	2.46E-06	1.76E-07	1.80E-07	1.88E-06
GA-ASA [11]	0.00E+00	1.73E-06	2.94E-06	4.54E-07	2.07E-07	2.02E-06
LADM [8]	0.00E+00	1.20E-09	5.89E-09	2.24E-08	9.09E-08	3.39E-07
LADM-Padé [8]	0.00E+00	1.20E-09	6.15E-09	5.78E-08	8.26E-08	1.21E-07
VIM [12]	0.00E+00	1.12E-09	4.23E-09	1.96E-07	2.20E-06	1.57E-05
MVIM [12]	0.00E+00	1.19E-09	5.29E-09	1.27E-08	2.27E-08	3.12E-08
HPM [7]	0.00E+00	1.20E-09	5.89E-09	2.24E-08	9.09E-08	3.39E-07
Bessel [9]	0.00E+00	2.16E-07	2.17E-07	8.58E-07	1.78E-06	3.09E-06

Table 10: Comparison of absolute errors for $V(t)$ of the proposed schemes and classical methods relative to RK4-method

t_i	0.0	0.2	0.4	0.6	0.8	1.0
LWCM	0.00E-00	1.00E-10	1.24E-06	1.15E-06	9.50E-07	7.61E-07
cGP(2)-method	0.00E+00	8.66E-07	1.07E-06	9.95E-07	8.21E-07	6.34E-07
GA [11]	0.00E+00	1.79E-05	1.03E-05	8.44E-06	1.28E-05	8.11E-06
IPA [11]	0.00E+00	1.32E-05	3.41E-06	3.03E-06	7.94E-06	6.64E-06
ASA [11]	0.00E+00	1.49E-05	8.39E-07	3.83E-06	7.02E-06	5.42E-06
GA-IPA [11]	0.00E+00	1.32E-05	3.40E-06	3.07E-06	7.91E-06	6.64E-06
GA-ASA [11]	0.00E+00	1.46E-05	1.49E-06	4.05E-06	7.03E-06	5.66E-06
LADM [8]	0.00E+00	1.00E-07	1.33E-05	2.15E-04	1.53E-03	6.95E-03
LADM-Padé [8]	0.00E+00	1.08E-07	1.84E-05	6.87E-04	4.71E-03	5.80E-03
VIM [12]	0.00E+00	1.00E-07	1.33E-05	2.16E-04	1.54E-03	6.98E-03
MVIM [12]	0.00E+00	5.61E-08	1.06E-06	5.75E-06	2.01E-05	5.64E-05
HPM [7]	0.00E+00	1.00E-07	1.33E-05	2.15E-04	1.53E-03	6.95E-03
Bessel [9]	0.00E+00	6.59E-08	3.79E-08	2.31E-07	7.87E-07	1.46E-02

6. Conclusion

The numerical solution of a comprehensive model for HIV infection of heathy T-cells has been presented using the cGP(2) and LWCM. We sought to determine the effect of constant and different variable source terms for supply of new healthy T-cells from thymus on HIV infection model. By presenting the results, it can be established that the dynamics of healthy T-cells, infected T-cells and free HIV virus particles behaves as a damped oscillating manner for all kind of source terms throughout the time period of seventy days but their are only an unsubstantial changes in their population rate. The change in concentration of $T(t)$, $I(t)$ and $V(t)$ are different for source term s_1 throughout the time period but for other source terms they have comparatively same in dynamical behavior at initial stages and the changes appear after some time.

13

In phase diagram all the source term show similarity in their dynamics for some time but after some time their population dynamics changes from each other. The population of virus and infected T-cells gradually increases from the first day of infection in the model with source term s_3 and the concentration of healthy T-cells increases, reach to maximum level and then decreases gradually. On the other hand, we solved the model by using RK4-method and present the quantitative comparison of cGP(2) and LWCM with other conventional methods for $T(t)$, $I(t)$ and $V(t)$. Finally, we depicted the numerically curves generated by cGP(2) and LWCM. We notice that cGP(2) and LWCM have approximately similar accuracy as compared to other methods used for the HIV infection model.

References

[1] S. Perelson, Mathematical and Statistical Approaches to AIDS Epidemiology, Springer–Verlag New York, Inc., New York, NY, USA, 1989.
URL http://dl.acm.org/citation.cfm?id=90146.90450

[2] A. Perelson, D. Kirschner, R. Boer, Dynamics of HIV infection of CD4$^+$ T-cells, Mathematical Biosciences 114 (1993) 81–125.

[3] M. Nowak, R.M. May, Virus dynamics, Oxford University Press.

[4] A. Perelson, P. Nelson, Mathematical analysis of HIV-1, dynamics in vivo, SIAM Rev 1 (41) (1999) 3–44.

[5] H. Hethcote, The mathematics of infectious diseases, SIAM Review (42) (2000) 599–653.

[6] R. Culshaw, S. Ruan, A delay differential equation model of HIV infection of CD4$^+$ T-cells, Mathematical Biosciences 165 (2000) 27–39.

[7] M. Medan, Homotopy perturbation method for solving a model for HIV infection of CD4$^+$ T-cells, Istanbul Tipcart Universities Fen Balmier Derris Yell 12 (2007) 39—-52.

[8] M. Ongun, The laplace adomian decomposition method for solving a model for HIV infection of CD4$^+$ T-cells, Mathematical and Computer Modeling 63 (2011) 597—-603.

[9] S. Yüzbas, A numerical approach to solve the model for HIV infection of CD4$^+$T-cells, Appl. Math. Model. (36) (2012) 5876—5890.

[10] M. Ghoreishi, A. Ismail, A. Alomari, Application of the homotopy analysis method for solving a model for HIV infection of CD4$^+$ T-cells, Mathematical and Computer Modeling 54 (2011) 3007—-3015.

[11] S. Malik, I. Qureshi, M. Amir, A. Malik, Nature inspired computational approach to solve the model for HIV infection of CD4$^+$T-cells, Research journal of recent sciences 3 (6) (2014) 67—-76.

[12] M. Merdan, A. Gökdoğan, A. Yildirim, On the numerical solution of the model for HIV infection of CD4$^+$T-cells, Comput. Math. Appl. (62) (2011) 118—123.

[13] X. Wang, X. Song, Global stability and periodic solution of a model for HIV infection of CD4$^+$ T-cells, Applied Mathematics and Computation 189 (2007) 1331–1340.

[14] N. Doğan, Numerical treatment of the model for HIV infection of CD4$^+$T-cells by using multistep laplace adomian decomposition method, Discrete Dynamics in Nature and Society (11).

[15] D. Kirschner, Using mathematics to understand HIV immune dynamics 43 (11) (1996) 191–202.

[16] D. Kirschner, S. Lenhart, S. Serbin, Optimal control of the chemotherapy of HIV, Journal of mathematical Biology 17 (35) (1997) 775–792.

[17] J. Hermández, J. García, D. Kirschner, Remarks on modeling host-pathogen systems.

[18] D. Kirschner, G. Webb, A model for HIV treatment strategy in the chemotherapy of AIDS, Bulletin of Mathematical Biology 58 (2) (1996) 367–390.

[19] S. Butler, D. Kirschner, S. Lenhart, Optimal control of chemotherapy affecting the infectivity of hiv, Ann Arbor 1001 (1997) 0620–48109.

[20] F. Schieweck, Astable discontinuous Galerkin-Petrov time discretization of higher order, J. Numer. Math 18 (2010) 25—57.

[21] S. Hussain, F. Schieweck, S. Turek, Higher order Galerkin time discretizations and fast multigrid solvers for the heat equation, Journal of Numerical Mathematics 19 (1) (2011) 41—61.

[22] S. Hussain, F. Schieweck, S. Turek, A note on accurate and efficient higher order Galerkin time stepping schemes for the nonstationary Stokes equations, The Open Numerical Methods Journal 4 (2012) 35–45.

[23] S. Hussain, F. Schieweck, S. Turek, Higher order Galerkin time discretizations and fast multigrid solvers for the heat equation, Journal of Numerical Mathematics 19 (1) (2011) 41—-61.

[24] S. Hussain, F. Schieweck, S. Turek, An efficient and stable finite element solver of higher order in space and time for nonstationary incompressible flow, Tech. rep., Fakultät für Mathematik, TU Dortmund, ergebnisberichte des Instituts für Angewandte Mathematik, Nummer 450 (2012).

[25] S. Hussain, F. Schieweck, S. Turek, Higher order Galerkin time discretizations and fast multigrid solvers for the heat equation, Tech. rep., Fakultät für Mathematik, TU Dortmund, ergebnisberichte des Instituts für Angewandte Mathematik, Nummer 416 (Nov. 2010).

[26] G. Matthies, F. Schieweck, Higher order variational time discretizations for nonlinear systems of ordinary differential equations, Preprint 23/2011, Otto-von-Guericke Universität Magdeburg, Fakultät für Mathematik (2011).

[27] M. Sohaib, S. Haq, S. Mukhtar, I. Khan, Numerical solution of sixth-order boundary-value problems using Legendre wavelet collocation method, Results in Physics 8 (2018) 1204–1208.

[28] S. Islam, I. Aziz, A. Fhaid, A. Shah, A numerical assessment of parabolic partial differential equations using Haar and Legendre wavelets, Applied Mathematical Modeling 37 (2013) 9455–9481.

[29] M. Heydari, M. Hooshmandasl, F. M. Ghaini, C. Cattani, Wavelets method for the time fractional diffusion-wave equation, Physics Letters A 379 (2015) 71–76.

[30] M. Heydari, M. Hooshmandasl, F. Ghaini, F. Fereidouni, Two dimensional legendre wavelets for solving fractional poisson equation with dirichlet boundary conditions, Engineering Analysis with Boundary Element 37 (2013) 1331–1338.

[31] M. Razzaghi, S. Yousefi, Legendre wavelet direct method for variational problems, Mathematics and Computers in Simulation 53 (2000) 185–192.

[32] A. Aziz, P. Monk, Continuous finite elements in space and time for the heat equation, Math. Comp 52 (186) (1989) 255–274.